

Plasmon-Assisted Optofluidics

Jon S. Donner,[†] Guillaume Baffou,^{†,‡,*} David McCloskey,[†] and Romain Quidant^{†,§,*}

[†]ICFO - Institut de Ciències Fotòniques, Mediterranean Technology Park, 08860 Castelldefels, Barcelona, Spain, [‡]Institut Fresnel, MOSAIC, CNRS, Aix-Marseille Université, Domaine Universitaire Saint-Jérôme, 13197 Marseille Cedex 20, France, and [§]Institució Catalana de Recerca i Estudis Avançats (ICREA), 08010 Barcelona, Spain

Gold nanoparticles supporting localized plasmon resonances can act as point-like nanosources of heat, remotely controllable by laser illumination.¹ Along with the fast growing interest in the biomedical field,^{2,3} nanoscale control of temperature⁴ opens up multiple new opportunities in nanotechnology including chemistry,⁵ phase transition,⁶ and material growth.⁷ Beyond this emerging research, another concept that has only marginally been addressed is the ability to exploit plasmonic nanoparticle heating to control fluid motion at the nanoscale.^{8,9} Controlling fluid dynamics using plasmonic heating is first motivated by the possibility of engineering fluid motion at the nanometer scale as a strategy to develop future elementary functionalities in micro- and nanofluidic experiments. Furthermore, since heating is intrinsic to plasmonic nanostructures, there are numerous optical experiments in which an undesired fluid motion could affect or interfere with the phenomenon under investigation. In that case, quantifying the temperature increase and the amplitude of the fluid velocity is crucial to discriminate between the different effects. As an example, let us mention the concept of plasmon-assisted trapping, where the enhanced optical field around single metal nanostructures is used to trap single tiny objects in solution.¹⁰ While prior studies have evoked that heat-induced fluid dynamics may contribute to plasmon-assisted trapping, there has not been any demonstration nor quantification of such contribution.

In this paper, we investigate theoretically and numerically the dynamics of the thermal-induced fluid convection around a gold structure under illumination. The objectives are to quantify the expected physical orders of magnitude and to discuss the feasibility of controlling fluids at the nanoscale using plasmonic structures. We restrict ourselves to the simple case of a gold nanostructure lying on a glass substrate and surrounded by water. To begin with, we develop the

ABSTRACT We study the ability of a plasmonic structure under illumination to release heat and induce fluid convection at the nanoscale. We first introduce the unified formalism associated with this multidisciplinary problem combining optics, thermodynamics, and hydrodynamics. On this basis, numerical simulations were performed to compute the temperature field and velocity field evolutions of the surrounding fluid for a gold disk on glass while illuminated at its plasmon resonance. We show that the velocity amplitude of the surrounding fluid has a linear dependence on the structure temperature and a quadratic dependence on the structure size (for a given temperature). The fluid velocity remains negligible for single nanometer-sized plasmonic structures (<1 nm/s) due to a very low Reynolds number. However thermal-induced fluid convection can play a significant role when considering either micrometer-size structures or an assembly of nanostructures.

KEYWORDS: plasmonics · optical heating · thermodynamics · hydrodynamics · nanoscale · microscale

theoretical framework required to describe the physics involved. Then, we carry out numerical simulations using a finite element method to compute the evolutions of the temperature and velocity fields of the fluid surrounding the gold structure. As much as we can, we perform dimensional analysis of the constitutive equations to show how the characteristic orders of magnitude—especially regarding time scale and fluid velocity—can be simply estimated analytically. This parallel approach gives estimations in very good agreement with the numerical simulations. We finally show how these results provide some insight into the actual contribution of thermal effects in plasmon-assisted trapping experiments.

RESULTS AND DISCUSSION

The thermo-induced fluid motion expected around a gold nanostructure under illumination originates from light absorption. When illuminated by a monochromatic light at angular frequency ω , the heat source density *inside* the gold structure originates from Joule effect and reads

$$q(\mathbf{r}) = \frac{\omega}{2} \text{Im}(\epsilon_{\text{Au}}) |\mathbf{E}(\mathbf{r})|^2 \quad (1)$$

where ϵ_{Au} is the gold permittivity. We use the following convention: $\mathbf{E}(\mathbf{r}, t) = \text{Re}\{\mathbf{E}(\mathbf{r})e^{-i\omega t}\}$

* Address correspondence to guillaume.baffou@fresnel.fr; romain.quidant@icfo.es.

Received for review February 14, 2011 and accepted June 9, 2011.

Published online June 09, 2011
10.1021/nn200590u

© 2011 American Chemical Society

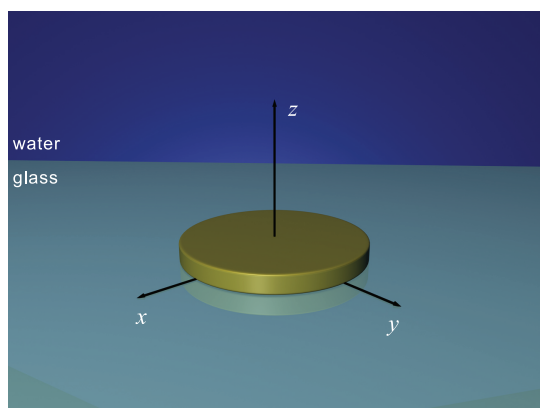


Figure 1. Geometry of the system investigated. It consists of a gold disk of height h_0 and radius r_0 lying on a planar glass substrate and immersed in water. The structure is illuminated from the bottom by a plane wave under total internal reflection.

is the electric field and $\mathbf{E}(\mathbf{r})$ its complex amplitude. The profile $q(\mathbf{r})$ inside the structure strongly depends on the geometry and can be highly non-uniform.^{11,12} This effect generates a temperature distribution $T(\mathbf{r}, t)$ inside the structure governed by the heat diffusion equation:

$$\rho_{\text{Au}} c_{\text{Au}} \partial_t T(\mathbf{r}, t) - \kappa_{\text{Au}} \nabla^2 T(\mathbf{r}, t) = q(\mathbf{r}) \quad (2)$$

where κ_{Au} is the thermal conductivity of gold, ρ_{Au} its density, and c_{Au} its specific heat capacity at constant pressure. Note that the temperature profile inside the structure is usually very uniform despite the non-uniformity of the heat source $q(\mathbf{r})$.^{4,12,13} This is due to much higher thermal conductivity of gold compared to that of water. Outside the structure, no heat is generated since the light absorption of water is negligible ($q(\mathbf{r}) = 0$), but some convection may occur. Hence, the temperature distribution in the surrounding water is governed by the following equation:

$$\rho c [\partial_t T(\mathbf{r}, t) + \nabla \cdot (T(\mathbf{r}, t) \mathbf{v}(\mathbf{r}, t))] - \kappa \nabla^2 T(\mathbf{r}, t) = 0 \quad (3)$$

where $\mathbf{v}(\mathbf{r}, t)$ is the fluid velocity and $\nabla \cdot (T\mathbf{v})$ is an additional nonlinear convective term. κ is the thermal conductivity of water, ρ its mass density, and c its specific heat capacity at constant pressure.

Due to the temperature increase that takes place within the fluid around the structure, the fluid experiences some reduction of its mass density, which yields an upward convection of the fluid (Archimedes force). The general equation governing this profile of the fluid velocity is the Navier–Stokes equation:¹⁴

$$\partial_t \mathbf{v}(\mathbf{r}, t) + (\mathbf{v}(\mathbf{r}, t) \cdot \nabla) \mathbf{v}(\mathbf{r}, t) = \nu \nabla^2 \mathbf{v}(\mathbf{r}, t) + \mathbf{f}_{\text{th}}(T(\mathbf{r}, t)) \quad (4)$$

where ν is the viscosity of water and \mathbf{f}_{th} the force per unit mass due to temperature non-uniformity. This thermal force can be estimated using the Boussinesq approximation.¹⁴ This approximation accounts for the temperature dependence of the mass density

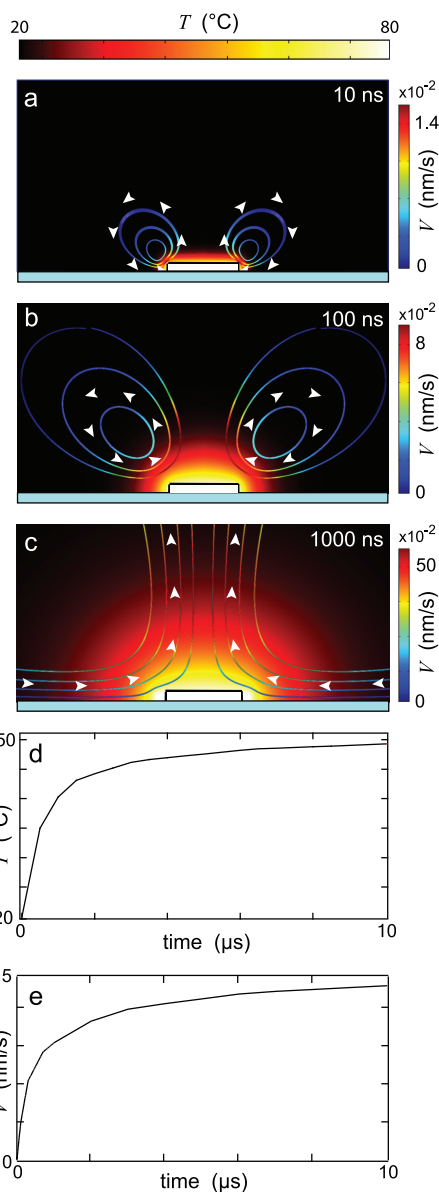


Figure 2. Temporal study of fluid convection around a gold disk, of height 40 nm and diameter 500 nm, which is heated at time $t = 0$ from room temperature to 80 °C. (a–c) Temperature and velocity patterns (stream lines) at different times. (d) Temperature of the liquid as a function of time, measured at a point located one radius (250 nm) above the gold disk. (e) Velocity of the liquid as a function of time, measured at the same point.

by adding an external buoyancy force term that is dependent on the temperature distribution:

$$\mathbf{f}_{\text{th}}(T) = \beta g \delta T(\mathbf{r}, t) \mathbf{u}_z \quad (5)$$

where g is the gravitational acceleration, β the dilatation coefficient of water, $\delta T(\mathbf{r}, t) = T(\mathbf{r}, t) - T_\infty$ the temperature increase, and \mathbf{u}_z the upward unit vector along the z direction.

Several numerical techniques^{4,13,15,16} have been developed to compute the temperature distribution around plasmonic structures, but none of them have been extended to take into account a possible

thermal-induced fluid convection as well. We chose to solve numerically in parallel eqs 1, 2, 3, 4, and 5 using Comsol Multiphysics, a commercial software based on finite element calculations and suited to address problems coupling several different differential equations (see Methods section). We consider a typical configuration consisting of a gold disk (radius r_0 and height h_0) lying on a planar glass substrate and surrounded by water (Figure 1). The structure is illuminated from the bottom by a monochromatic light at the angular frequency ω .

As a first step, we perform simulations in which we simply consider the inner temperature increase of the gold disk T_0 as a parameter. Hence, eq 2 is not solved in this part. Considering the temperature of the gold structure as uniform is justified owing to the very high thermal conductivity of gold compared to water, as mentioned above.^{4,12,13} The temperature is varied over the possible physical values: from $T_\infty = 20$ °C, the room temperature, up to 100 °C, the boiling point. Note that, in order to retrieve the actual temperature increase T_0 from the knowledge of the light irradiance (a physical quantity easier to estimate experimentally), we provide simple analytical expressions in ref 4 for a wide set of structure sizes and geometries.

Figure 2 addresses the dynamical properties of the thermal-induced convection. The inner temperature increase T_0 of the disk, applied at time $t = 0$, results in a laminar regime and a Rayleigh–Benard-like fluid convection around the disk, as can be seen in the velocity profiles in Figure 2a–c. Figure 2d plots the evolution of the temperature of the fluid—measured one radius above the structure (250 nm)—as a function of time. Figure 2e plots the evolution of the velocity of the fluid—measured at the same location—as a function of time. Interestingly, these two profiles are very similar in shape and in characteristic times. This can be explained by dimensional analysis of eqs 3 and 4. These two equations are mathematically identical (if one discards the nonlinear convective terms): they are diffusion equations. The time scales associated with these equations are respectively

$$\tilde{t}_T = \tilde{L}^2/\alpha \quad (6)$$

$$\tilde{t}_v = \tilde{L}^2/\nu \quad (7)$$

\tilde{L} is the characteristic size of the plasmonic structure, \tilde{t}_T is the characteristic time related to the establishment of the steady-state temperature profile, and \tilde{t}_v is the one related to the establishment of the steady-state velocity profile. $\alpha = \kappa/\rho c$ is the water diffusivity. Both these parameters have the dimension of a diffusion coefficient (m^2/s^{-1}). Coincidentally, α and ν are on the same order of magnitude ($\alpha = 0.14 \times 10^{-6}$ and $\nu \approx 0.3 \times 10^{-6}$ to 1.0×10^{-6} m^2/s). This is the reason that the temperature and the velocity determinations occur over the same time scale ($\tilde{t}_T \approx \tilde{t}_v$). In general, in

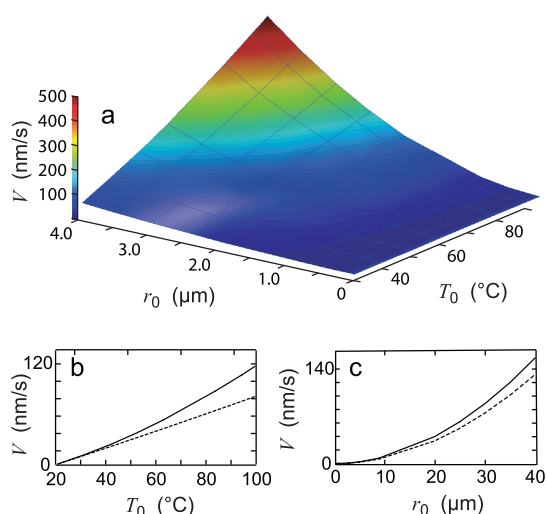


Figure 3. Influence of the disk temperature and the disk diameter on the velocity magnitude. (a) Map representing the velocity measured at a point located one diameter above the disk, as a function of the disk temperature and the disk radius. (b) Velocity as a function of the disk temperature for $r_0 = 2$ μm . (c) Velocity as a function of the disk radius for $T_0 = 50$ °C. (The dashed lines are the results of the calculations when the water coefficients are constant and do not depend on the temperature.)

nanoplasmonics experiments, these time scales are on the order of 1 ns to 1 μs depending on the size of the structure. In this particular case, the characteristic length of the system is the radius of the disk, $R = 250$ nm; this yields $\tilde{t}_T \approx 0.5$ μs and $\tilde{t}_v \approx 1$ μs , which is in very good agreement with the numerical simulations, for which exponential fits of Figure 2d,e give $\tilde{t}_T \approx 0.4$ μs and $\tilde{t}_v \approx 0.8$ μs . Note that the time scales are not dependent on the temperature increase.

Figure 3 depicts the influence of the disk temperature increase T_0 and the disk radius r_0 on the velocity field magnitude. In Figure 3b, the fluid velocity is plotted for two conditions: when the fluid parameters (κ , c , ν , ρ) are kept constant (independent of the temperature) (dashed line) and when their variation as a function of temperature is taken into account (solid line). In the first case, a perfect linear variation is observed despite the nonlinear terms $\nabla(\mathbf{T}\mathbf{v})$ and $(\mathbf{v}\cdot\nabla)\mathbf{v}$ present in the two constitutive equations, eqs 3 and 4, respectively. One can show by dimensional analysis that these two terms are indeed expected to be negligible and that this problem can be described by linear equations:

First, in eq 4, we have a convective term $(\mathbf{v}\nabla)\mathbf{v}$, diffusive term $(\nu\nabla^2)\mathbf{v}$, and the force (\mathbf{f}_{th}). The orders of magnitude of these three terms are respectively \tilde{V}^2/\tilde{L} , $\nu\tilde{V}/\tilde{L}^2$, and $\beta g T_0$, where \tilde{V} is the order of magnitude of the fluid velocity, \tilde{L} the characteristic size of the plasmonic structure, and T_0 its temperature increase. The dynamics is driven by the force \mathbf{f}_{th} . The question is whether the diffusive term or the convective term is dominant. By equating these three orders of magnitude, we find that the transition from a diffusive to a

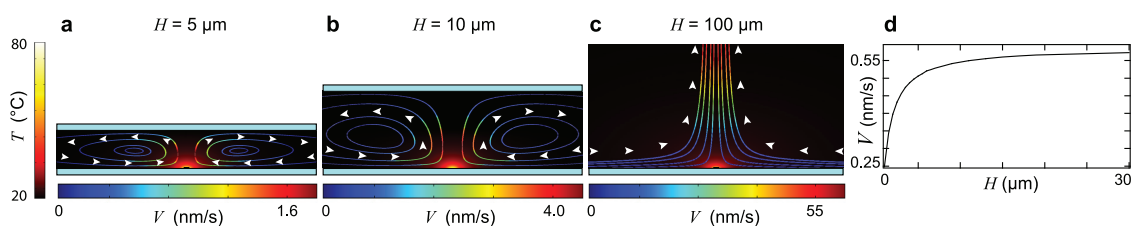


Figure 4. Investigation of the influence of chamber height on thermally induced fluid motion in plasmon-assisted trapping experiments. (a–c) Velocity fields for various chamber heights H , induced by a gold disk of radius $r_0 = 250$ nm and $T_0 = 80$ °C. (d) Velocity as a function of H , measured at one radius (250 nm) above the disk.

convective regime would occur at $T_0 \approx \nu^2/\tilde{L}^3\beta g$. This is on the order of 10^6 to 10^9 K, which is nonsense. Incidentally, whatever the temperature of the structure, the dynamics will be necessarily driven by the diffusive term and the convective term will be negligible (no turbulent flow is expected). By equating the orders of magnitude of the remaining diffusive and force terms we can now estimate the order of magnitude of the velocity of the fluid induced by a structure of typical size \tilde{L} and temperature increase T_0 :

$$\tilde{V} = \tilde{L}^2\beta g T_0/\nu \quad (8)$$

For $\tilde{L} = 250$ nm (radius of a disk) and a temperature increase of $T_0 = 60$ °C, and using $\rho = 10^3$ kg/m³, $\beta = 10^{-4}$ K⁻¹, $\nu = 10^{-6}$ Pa·s, and $g = 9.8$ m/s², we obtain a characteristic fluid velocity of the thermal-induced convection of $\tilde{V} \approx 10^{-9}$ m/s. This is in very good agreement with numerical calculations presented in Figure 2e. One can now compare the order of magnitude of the nonlinear (convective) term with the diffusion term of eq 4. The ratio of these two quantities is called the Reynolds number, Re. This gives

$$\text{Re} = \frac{\tilde{V}\tilde{L}}{\nu} = \frac{\beta g T_0 \tilde{L}^3}{\nu^2} \quad (9)$$

A fluid flow associated with small Reynolds number (<0.1) is governed by viscous forces and is laminar, whereas high Reynolds numbers are associated with turbulent fluid flows. In our case, $\text{Re} \approx 10^{-8}$, which refers to a highly viscous and laminar fluid motion.

Second, in eq 3, $\rho c \nabla(\mathbf{T}\mathbf{v})$ represents heat transport through fluid convection, on the order of $\rho c T_0 \tilde{V}/\tilde{L}$, while $\kappa \nabla^2 T$ represents heat transport through heat diffusion, on the order of $\kappa T_0/\tilde{L}^2$. The ratio of these orders of magnitude gives a dimensionless number—called the Rayleigh number (Ra)¹⁴—that quantifies the heat diffusion *versus* heat convection effects:

$$\text{Ra} = \frac{\tilde{V}\tilde{L}}{\alpha} = \frac{\beta g T_0 \tilde{L}^3}{\alpha \nu} \quad (10)$$

If the Rayleigh number Ra is much lower (respectively larger) than unity, thermal diffusion is dominant (respectively negligible) with respect to fluid convection on the establishment of the temperature profile.

In the present case, $\text{Ra} \approx 10^{-7}$, which shows that the nonlinear term of eq 3 is indeed negligible. As a consequence, in nanoplasmonics experiments occurring in water-like medium, the temperature distribution is mainly governed by heat diffusion and not fluid convection. In other words, on the nanoscale the temperature reaches its steady-state distribution so fast that such a slow fluid motion ($\tilde{V} \approx 10^{-9}$ m/s) cannot distort it. The evolution of the temperature profile around the structure is the same as if the fluid were not moving.

Consequently, in a problem involving thermo-induced fluid convection at the nano- or microscale, calculations in the surrounding water can be performed in a very good approximation by considering the set of linear diffusion equations:

$$\partial_t T(\mathbf{r}, t) - \alpha \nabla^2 T(\mathbf{r}, t) = 0 \quad (11)$$

$$\partial_t \mathbf{v}(\mathbf{r}, t) - \nu \nabla^2 \mathbf{v}(\mathbf{r}, t) = \mathbf{f}_{\text{th}}(T(\mathbf{r}, t)) \quad (12)$$

Incidentally, note that the problem consisting of computing the temperature profile evolution and the velocity profile evolution is not self-consistent. Equation 11 can be resolved first to obtain the evolution of the temperature profile, and then the velocity profile can be computed using eq 12.

Regarding the influence of the disk size (Figure 3c), the main conclusion is that varying the disk radius has a quadratic effect on the velocity field, as predicted by eq 8. Incidentally, if a fluid motion is wanted, the size of the structure is a more sensitive parameter than the laser power: if the size of the structure is doubled, the fluid velocity is multiplied by a factor of 4 (for a given temperature of the structure). However, for nanometric structures (typically of size below 200 nm), even for temperatures close to the boiling point, the fluid velocity hardly exceeds 10 nm/s, as shown in Figure 3a. As a consequence, any molecular motion will be mainly driven by Brownian dynamics or thermophoresis. In this case, isolated plasmonic nanoparticles will not be efficient to control micro- and nanofluidics, for instance molecular drift. Faster fluid motion (hundreds of nanometers per second) can be achieved only when using structures typically bigger than 1 or 2 μm. Note that increasing the size of the gold structure may lead to undesired red-shift of its plasmonic resonance. This

problem can be circumvented by using *assemblies* of nanoparticles, as in ref 8. In this case, the typical size \tilde{L} of the hot area becomes the size of the array, which can be taken as large as necessary to induce fast fluid motion, and this approach will not affect the resonance wavelength of the nanoparticles that will remain in the desired visible or near-infrared range. This paradigm is intrinsically more complicated to design and build, but could allow for more control over micro- and nanofluidics.

It has recently been proposed to exploit enhanced plasmonic fields to optically trap micro- and nano-objects at a surface patterned with gold structures.^{10,17} Under illumination, plasmonic structures are surrounded by a large electric field gradient that creates a stable optical potential well for a nearby specimen. When this kind of trap was reported,¹⁰ it was evoked that fluid convection due to heating of the plasmonic structure could *a priori* play a role in the trapping process. However, it was not possible to quantify this contribution. In this part, we address the matter of the contribution of thermal-induced fluid motion in plasmon-assisted trapping experiments. The main question is to figure out whether this centripetal velocity field observed in the previous paragraph is strong enough to play a role in the trapping process as compared to optical forces. In this work,¹⁰ the gold disks were $2\ \mu\text{m}$ in diameter and $40\ \text{nm}$ in height. The laser irradiance was $5 \times 10^{-2}\ \text{mW}/\mu\text{m}^2$ in total internal reflection from the glass substrate. The trapping disks were immersed in water in a chamber of height $10\ \mu\text{m}$.

We carried out numerical simulations using Comsol Multiphysics under the same conditions (see Methods section). We found that the disk temperature increases by about $6\ ^\circ\text{C}$, leading to a maximum velocity on the order of $1\ \text{nm/s}$. Incidentally, in plasmon-assisted trapping experiments, the fluid convection is so slow that it definitely cannot contribute to the trapping effect. This result supports the all-optical origin of the trapping effect proposed in ref 10. Another phenomenon that could *a priori* come into play in the trapping dynamics is the Soret effect, also called thermophoresis.¹⁸ This phenomenon happens when an object (molecule or particle) immersed in a liquid is subject to a temperature gradient. It usually yields a motion from hot

to cold regions, but the effect can reverse for very small objects (molecules) and low temperatures (a few degrees). In the present case, given the size of the object and the temperature range, any thermophoresis contribution should push the beads from hot to cold places. Consequently, thermophoresis cannot contribute to any trapping process in the above-mentioned experiment.

Another interesting parameter that we finally discuss is the influence of the height, H , of the liquid chamber on the liquid dynamics. In a fluidic environment, a top cover slide is usually added to confine the liquid in the z direction. The chamber height can eventually decrease to a few micrometers. This dependence was also studied numerically and is presented in Figure 4. As can be seen, below a certain height the velocity field can be damped by more than 1 order of magnitude. Consequently, the fluid confinement is also a parameter that has to be considered when evaluating the magnitude of plasmonics-assisted fluid convection. When any fluid motion is to be avoided in a given experiment, the chamber height is a parameter that can be varied and minimized advantageously.

CONCLUSION

To summarize, by numerical simulations using Comsol and systematic dimensional analysis, we have investigated the physics of fluid convection induced by heat release arising from a metal nanostructure illuminated at its plasmonic resonance. We evidenced a laminar regime and a Rayleigh–Benard-like fluid convection. The characteristic time and velocity have been derived as a function of the size of the structure and its temperature increase. Transient evolutions last from $1\ \text{ns}$ to $1\ \mu\text{s}$ depending on the size of the structure but not on the temperature increase. We have shown that the thermal and hydrodynamic problems are not self-consistent and can be treated independently due to a low Rayleigh number. For isolated nanometric structures (below $200\ \text{nm}$) the Reynolds number is so low, even for temperatures close to the boiling point, that any plasmon-assisted fluid motion hardly exceeds $10\ \text{nm/s}$. To reach a few hundreds of nanometers per second and open the path for micro- and nanofluidics applications, larger structures have to be used, typically above $1\ \mu\text{m}$.

METHODS

Finite Element Method Analysis. We used the Comsol Multiphysics finite element modeling software. Due to axial symmetry of the system investigated, a two-dimensional model was considered. The Paradiso solver was used on a free triangular mesh. The heat transfer (ht) and laminar flow (spf) modules were used to solve eqs 2, 3, 4, and 5. The electromagnetic wave (rfw) module was used when solving eq 1. The physical parameters of gold, glass, and water were taken from the Comsol library, and their dependence on temperature was taken into account. Open boundaries are considered for the fluid flow and set at room

temperature. The size of the system is $r_{\text{max}} = 50\ \mu\text{m}$ and $z_{\text{max}} = 50\ \mu\text{m}$. The glass substrate is modeled as an insulating wall as well as the top coverslip in Figure 4. When solving eq 1 with the rfw module to compute the heat source density inside a given structure, spherical PML (perfectly matching layers) were used to avoid unphysical reflections on the boundaries of the system. The illumination consisted of a monochromatic plane wave coming from the glass side in total internal reflection at 62° .

Acknowledgment. This work was partially supported by the Spanish Ministry of Sciences under grants FIS2010-14834 and

CSD2007-046-NanoLight.es, the European Community's Seventh Framework Program under grant FP7-ICT-248835 (SPEDOC), and Fundació Privada CELLEX.

REFERENCES AND NOTES

1. Govorov, A. O.; Richardson, H. H. Generating Heat with Metal Nanoparticles. *Nano Today* **2007**, *2*, 30–38.
2. Jain, P. K.; El-Sayed, I. H.; El-Sayed, M. A. Au Nanoparticles Target Cancer. *Nano Today* **2007**, *2*, 18–29.
3. Lal, S.; Clare, S. E.; Halas, N. J. Nanoshell-Enabled Photothermal Cancer Therapy: Impending Clinical Impact. *Acc. Chem. Res.* **2009**, *41*, 1842–1851.
4. Baffou, G.; Quidant, R.; García de Abajo, F. J. Nanoscale Control of Optical Heating in Complex Plasmonic Systems. *ACS Nano* **2010**, *4*, 709–716.
5. Nitzan, A.; Brus, L. E. Theoretical Model for Enhanced Photochemistry on Rough Surfaces. *J. Chem. Phys.* **1981**, *75*, 2205–2214.
6. Challener, W. A.; Peng, C.; Itagi, A. V.; Karns, D.; Peng, W.; Peng, Y.; Yang, X. M.; Zhu, X.; Gokemeijer, N. J.; Hsia, Y.-T.; *et al.* Heat-Assisted Magnetic Recording by a Near-Field Transducer with Efficient Optical Energy Transfer. *Nat. Photon* **2009**, *3*, 220–224.
7. Cao, L.; Barsic, D.; Guichard, A.; Brongersma, M. Plasmon-Assisted Local Temperature Control to Pattern Individual Semiconductor Nanowires and Carbon Nanotubes. *Nano Lett.* **2007**, *7*, 3523–3527.
8. Miao, X.; Wilson, B. K.; Lin, L. Y. Localized Surface Plasmon Assisted Microfluidic Mixing. *Appl. Phys. Lett.* **2008**, *92*, 124108.
9. Liu, G. L.; Kim, J.; Lu, Y.; Pee, L. P. Optofluidic Control Using Photothermal Nanoparticles. *Nat. Mater.* **2006**, *5*, 27–32.
10. Righini, M.; Zelenina, A. S.; Girard, C.; Quidant, R. Parallel and Selective Trapping in a Patterned Plasmonic Landscape. *Nat. Phys.* **2007**, *3*, 477–480.
11. Baffou, G.; Quidant, R.; Girard, C. Heat Generation in Plasmonic Nanostructures: Influence of Morphology. *Appl. Phys. Lett.* **2009**, *94*, 153109.
12. Baffou, G.; Girard, C.; Quidant, R. Mapping Heat Origin in Plasmonic Structures. *Phys. Rev. Lett.* **2010**, *104*, 136805.
13. Baffou, G.; Quidant, R.; Girard, C. Thermoplasmonics Modeling: A Green Function Approach. *Phys. Rev. B* **2010**, *82*, 165424.
14. Guyon, E.; Hulin, J. P.; Petit, L.; Mitescu, C. D. *Physical Hydrodynamics*; Oxford University Press: USA, 2001.
15. Ekici, O.; Harrison, R. K.; Durr, N. J.; Eversole, D. S.; Lee, M.; Ben-Yakar, A. Thermal Analysis of Gold Nanorods Heated with Femtosecond Laser Pulses. *J. Phys. D: Appl. Phys.* **2008**, *41*, 185501.
16. Novotny, L.; Bian, R. X.; Xie, X. S. Theory of Nanometric Optical Tweezers. *Phys. Rev. Lett.* **1997**, *79*, 645.
17. Righini, M.; Ghenuche, P.; Cherukulappurath, S.; Myroshnychenko, V.; García de Abajo, F. J.; Quidant, R. Nano-Optical Trapping of Rayleigh Particles and Escherichia Coli Bacteria with Resonant Optical Antennas. *Nano Lett.* **2009**, *9*, 3387–3391.
18. Duhr, S.; Braun, D. Why Molecules Move along a Temperature Gradient. *Proc. Natl. Acad. Sci. U. S. A.* **2006**, *103*, 19678–19682.